International Symposium
On Turbulence and Shear Flow
Phenomena (TSFP-9)
June 30 - July 3, 2015 *Melbourne, Australia*

STUDY ON GRAPHICAL STATISTICS CHARACTERIZING A TURBULENT SCALAR DIFFUSION TOWARD THE SOURCE ESTIMATION VIA IMAGE PROCESSING

Daichi SEKINE
Department of Mechanical Engineering
Tokyo University of Science
2461 Yamazaki, Noda-shi, Chiba-ken, 278-8510, Japan
j7510069@ed.tus.ac.jp

Takahiro TSUKAHARA and Yasuo KAWAGUCHI
Department of Mechanical Engineering
Tokyo University of Science
2461 Yamazaki, Noda-shi, Chiba-ken, 278-8510, Japan
tsuka@rs.tus.ac.jp, yasuo@rs.tus.ac.jp

ABSTRACT

The objective of this research is to propose and evaluate a source location estimation method for turbulent diffusion based on limited data obtained in the downstream location. The problem is challenging considering the chaotic nature of turbulent fluctuation in addition to that the character of the problem belongs to the "inverse analysis".

The proposed method was applied to the experimental data of instantaneous concentration distribution obtained by PLIF (Planar Laser Induced Fluorescence) imaging in a center of water channel where the turbulent velocity field is approximately homogeneous. The proposed method takes 4 steps as follows. 1) Extract high-concentration patches from the instantaneous concentration distribution obtained at x by binaryzation. And then the patches are labeled 2) The dimensionless areas of the patches are statistically processed to obtain PDF (Probability density function) and calculate kurtosis Ku of the distribution. 3) Introduce the hypothesis that the kurtosis has the linear relationship to the streamwise location x. 4) Based on the hypothesis, turbulent diffusion source can be estimated.

As the above method is constructed based on an empirical relation, its availability must be verified. Moreover, from the chaotic nature of the turbulence, the availability of the method will be largely affected by the size of the obtained data and location where the data are taken. In the final part of this paper, relative error of the proposed method was estimated for variety of data size and locations. As the result of estimation, relative error of source location is around 20% except for the location in the vicinity to the source and unaffected by the data size (i.e. number of binarized PLIF pictures) in the range of 10 to 300 instantaneous binarized pictures of instantaneous concentration distribution whose data size is 0.13 megabyte per one frame. On the assumption that 20% of relative error is acceptable, the proposed method is applicable to the location of $T^*>25$ (T^* is the non-dimensional time, which corresponds to the streamwise location x) and image data size larger than 10 frames (0.13×10 megabyte).

INTRODUCTION

Contaminant released into the environment, either accidentally or deliberately, brings great threats to human beings. Over the past decades, determining the emission source of a contaminant has come to be a topic of intensive research due to its potential benefits worldwide for problems such as atmospheric pollution, water pollution and ocean pollution etc. Many researches have been devoted to source estimation method. Zhang et al. (2007) used inverse computational fluid dynamics modeling to locate contaminant sources in a two-dimensional aircraft cabin and in a three-dimensional office and improved the numerical stability by applying quasi-reversibility equation. However, this application can't ensure accurate source estimation in flow field where diffusion term is dominant. Islam (1992) used analytic solutions of Gaussian plume model for source estimation, which is a simple dispersion model of pollutants and limits its application only to the cases of steady conditions of dispersion in the atmosphere. Bagtzoglou et. al. (1999) employed reversed time random particle method to identify sources of contamination in groundwater systems, however, without considering the influence brought by turbulent diffusion. By mimicking blue crabs locating food and mates in the river, Webster et. al. (2011) addressed the problem of source location identification through sensor-mediated plume tracking and a developed control algorithm, with the performance comparing favorably to that of blue crabs, while at a fairly rapid speed. Oyagi et al. (2013) performed experiments of single point source set in the middle of a turbulent channel flow and estimated the source location from instantaneous concentration distribution based on the empirical correlation and Taylor's diffusion theory. However, the estimation from the instantaneous information, or a

concentration distribution on an arbitrary spanwise axis, did not have enough precision.

The objective of this research is to propose and evaluate a source location estimation method for turbulent diffusion based on limited data obtained in the downstream location. PLIF technique and special image processing methods are resorted to for this purpose. In what follows, the experimental apparatus and the research method are introduced followed by the image processing introduction. After that, the results of this research are given as well as some analysis and discussions. Finally is the conclusion.

EXPERIMENTAL APPARATUS AND METHODS

Experimental apparatus

Figure 1 shows the apparatus of a closed circulated two-dimensional channel employed to the present experiment. Water heated to 25℃ in the tank is pumped into the pipe at a constant flow rate and then passes through a honeycomb rectifier to become homogeneous before rushing into a flume with a rectangular cross section. The flow develops over a 2000 mm distance before encountering the dye source which is located on the flume centerline at the beginning of the measurement section (see Fig. 2). An electromagnetic flowmeter is installed for flowrate measurement. The flume is made of transparent acrylic resin to improve optical clarity and the aspect ratio of the rectangular cross section is 1:12.5 with the inner height (2δ) being 20 mm. The entire length of the flume is 4300 mm and the dye source location is designated to be at x=0.

Figure 2 gives the details of the imaging apparatus, including a dye injecting nozzle, a CW-YAG laser, a high speed camera, a color filter and a personal computer besides the measurement section. Rhodamine-WT is introduced as the fluorescent dye to simulate scalar diffusion. The laser focuses and scans laser beam across the test section through the sidewalls of the flume. The color filter is used to cut off unwanted fluorescence. The camera is mounted below the test section to capture digital images, which are simultaneously transferred to the computer and saved. Details of the experiment are listed in Table 1, with Reynolds number based on the inner height of the flume, the dynamic viscosity of water and the bulk mean velocity.

As the distance between the inlet of the flume and the measurement section is 2000 mm, which is long enough for the flow to become fully turbulent, meanwhile, the ratio of width to height of the flume is 12.5, large enough to neglect the effect of side walls, it is assumed that the measured turbulent flow is steady as well as homogeneous.

Methods

Planar laser-induced fluorescence technique is used. The fluorescent dye is injected into the turbulent flow at a rate controlled by a micro syringe pump to ensure its velocity identical with the bulk mean velocity of the flow, with an acceptable deviation below 1%. Plume images are collected in the measurement section with a high-speed camera. PLIF measurements are conducted at different distances downstream from the nozzle tip to investigate the diffusion phenomena of different diffusion time or

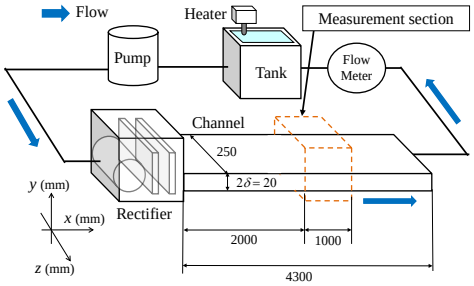

Figure 1 Experimental apparatus.

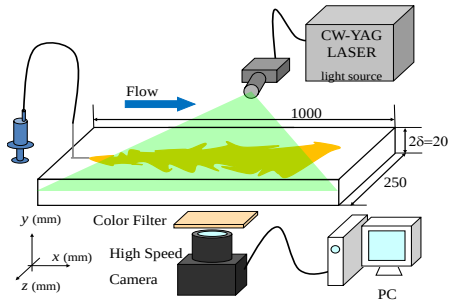

Figure 2 Imaging apparatus.

Table 1 Experimental conditions

Working fluid	Water (25 ℃)
Reynolds number	Re =2δU_b/ν = 20000
Dye	Rhodamine-WT
Laser	CW-YAG
Camera	Photoron: FASTCAM-APX RS 250K
Frame rate	3000 fps
Shutter speed	1/3000 sec
Diffusion time	T^* = 10, 25,30, 35,40,45,60

distances.

Diffusion time T is defined as,

$$T = \frac{x}{U_b} \tag{1}$$

x is the distance between the imaging area and the point source, U_b is the bulk velocity of turbulent flow.

Normalizing Eq. (1) by δ/U_b, the dimensionless diffusion time is thus expressed as,

$$T^* = \frac{T}{\delta / U_b} = \frac{x}{\delta} = x^* \tag{2}$$

Equation (2) shows that the dimensionless diffusion time here is identical with the dimensionless diffusion distance from the point source. However, the identical here can only be regarded as equality in value, as dimensionless diffusion distance is independent of bulk velocity while dimensionless diffusion time contains U_b. Thus, to be general, dimensionless diffusion time is chosen as the reference quantity.

Image processing

The images captured by the camera contain spatial information of the fluorescence intensity in the image area, which can reflect the spatial dye concentration distribution. Binaryzation image processing and concentration labeling are performed for the raw images successively. Binaryzation method proposed by Otsu is adopted here, which has the advantage of determining thresholds automatically and thus avoiding arbitrariness in image analyzing. By binaryzation, the spatial concentration distribution is regularized as two value levels, 0 for the black region and 255 for the white region. Through labeling, one is able to recognize and isolate the dye patches in the binary images, and thus obtain the shapes of the dye patches.

Fractal dimension

For fractals, there are no characteristic lengths which can distinguish their shapes and meanwhile ensure self-similarity of the shapes. The cloud in atmosphere and the marbling print in turbulent flow are something like fractals in this aspect. For fractals, fractal dimension is introduced as a measure of the shape, and the fractal dimension is 1.3~1.35 for cloud or turbulent marbling print.

Fractal dimension can be estimated by several methods. In this study fractal measurement is used which can generalize either a length quantity or area quantity of a fractal. Generally speaking, if an object of length L, area S and volume V is presumed, by dimension analysis, one can have,

$$L \propto S^{\frac{1}{2}} \propto V^{\frac{1}{3}} \tag{3}$$

Equation (3) can also be generalized as,

$$L \propto S^{\frac{1}{2}} \propto V^{\frac{1}{3}} \propto X^{\frac{1}{D_f}} \tag{4}$$

with X being a generalized quantity, and D_f being designated for fractal measurement and called the fractal dimension of X. Thus,

$$S^{\frac{1}{2}} \propto X^{\frac{1}{D_f}} \tag{5}$$

With S and X normalized by the flume half height, δ, and application of logarithm operation on both sides, Eq. (5) transforms to,

$$\mathbf{log}\, S^* = \frac{2}{D_f} \mathbf{log}\, X^* \tag{6}$$

In the following section, D_f is to be quantified through analysis of experiment results.

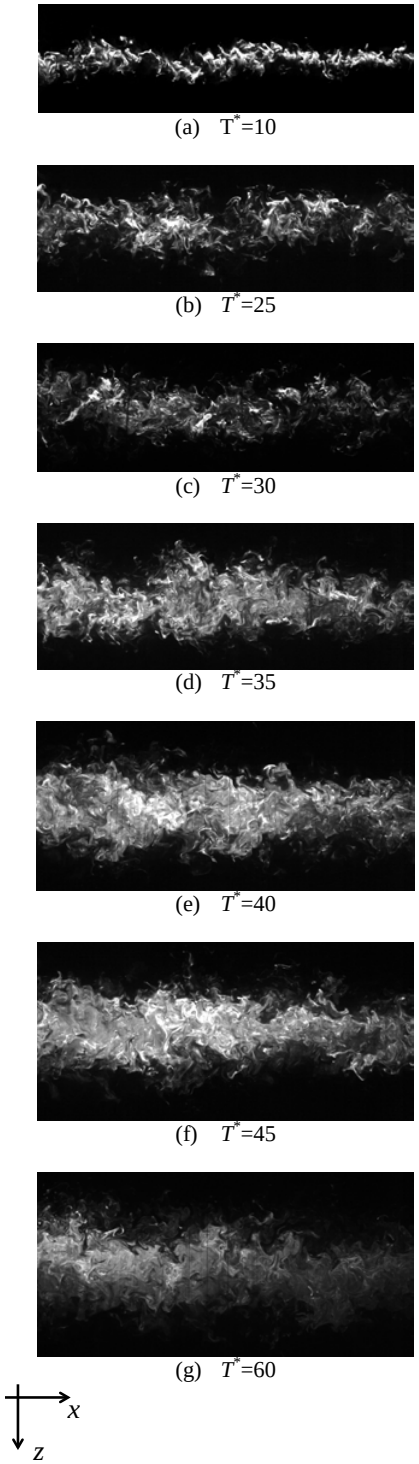

Figure 3 Raw images of dye diffusion.

RESULTS AND DISCUSSIONS

Experimental results

Figure 3 shows the raw images of dye diffusion by PLIF technique at different diffusion time.

As fluorescence intensity is proportional to dye concentration, high brightness in the images means high concentration of dye and vice versa. The turbulent diffusion of fluorescence dye can be seen clearly in Fig. 3,

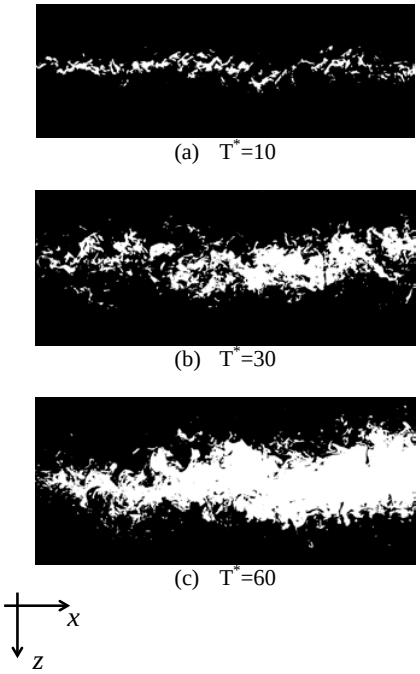

Figure 4 Binary images of dye diffusion.

from (a) to (g), obvious turbulent plume expanding in z direction is observed as magnified by the bright domain.

Then each raw image of dye diffusion is processed through binaryzation and the binary images are partly given in Fig. 4, taking cases of T^* = 10, T^* = 30 and T^* = 60 for example. Although fluctuation and distribution information of the dye concentration are removed by binaryzation, the general shape of high-concentration dye patch can be revealed and the deformation features of turbulent plume is preserved. Moreover, binaryzation process can simplify image analysis greatly and the noise in the images is rejected. Also the data size of obtained binary images is about 0.13 megabyte per one frame.

Relation of graphical turbulent statistics of single image and diffusion time

In our final goal of estimating the source location by using limited data in time and space, we studied graphical statistics which obtained by single image.

After binaryzation, the shapes of dye patches with relatively high concentration are recognized through labeling based on binary images. The dimensionless perimeter (=X^*) and area (=S^*) of each isolated dye patch are obtained, both normalized by flume half height δ. The logarithmic relationship of S^* and X^* for T^* = 10, T^* = 30 and T^* = 60 is plotted as a set of scattered circles shown in Fig. 5. A linear distribution is demonstrated, with the slope independent of the diffusion time. By Eq. (6), D_f for T^* = 10, 25, 30, 35, 40, 45 and 60 is calculated and plotted against T^*, as is shown in Fig. 6. All the dots are found around D_f = 1.35 marked by the red line and it is concluded that the fractal dimension is independent of the diffusion time, that is to say, the fractal dimension cannot be used for diffusion source estimation.

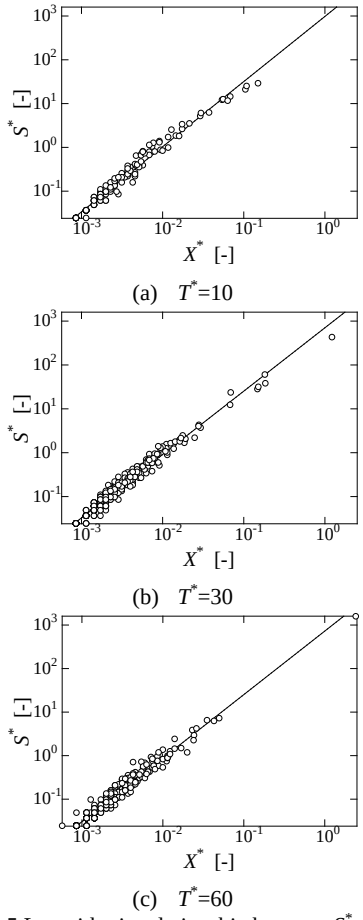

Figure 5 Logarithmic relationship between S^* and X^*.

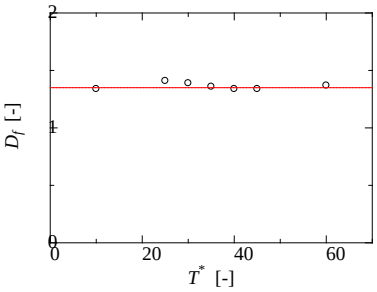

Figure 6 Fractal dimension distribution for different diffusion time.

Proposal of estimation method of diffusion time from graphical statistics of multiple images

However, from a statistic perspective, there is another important observation from Fig. 5 that is the detailed distribution of the circles for different diffusion time varies obviously. To have a deep knowledge, based on Eq. (7), each PDF of log (S^*) from statistical sampling analysis of 500 images is plotted as red dots shown in Fig. 7 for T^* = 10, T^* = 30 and T^* = 60. Meanwhile, the dots are fitted by black solid curves with least square method.

$$p\,(a \le S^* \le b) = \int_a^b P\,(S^*)\,dS^* \qquad (7)$$

Figure 7 shows how the PDF curve changes as diffusion time increases: an obvious shift of the peak location towards left side of log (S^*) coordinate, along with a sharpened distribution are demonstrated. Quantitatively speaking, the kurtosis (= *Ku*) of the PDF curve changes with diffusion time. To reveal this phenomenon, the kurtosis at each diffusion time is averaged by 500 images, and the results are plotted against diffusion time as shown in Fig. 8. It is noted that the kurtosis, *Ku*, increases approximately linearly as a function of the diffusion time. Through least square approach, the formula expressing the relationship between diffusion time and kurtosis was obtained,

$$T^* = 35Ku - 65 \qquad (8)$$

Equation (8) makes it possible to estimate the diffusion time directly from PDF kurtosis.

Besides the above mentioned, Fig. 7 also indicates that log (S^*) tends to remain at a certain value region. Taking Fig. 7 (c) for example, it is noted that most of log (S^*) appears around -3.4. Based on the bulk Reynolds number (20000 in our experiment), the friction Reynolds number can be described as $\mathbf{Re}_\tau = \frac{u_\tau \delta}{\nu} \approx 400$ (u_τ is friction velocity), and thus we have,

$$\sqrt{S} = \frac{\delta}{10^{1.7}} = 8.0 \times \frac{\nu}{u_\tau} \qquad (9)$$

For comparison, Kolmogorov scale at $Re_\tau \approx 400$ was formulated as,

$$\eta = 4.5 \times \frac{\nu}{u_\tau} \qquad (10)$$

Comparison of Eq. (9) and (10) reveals that $\sqrt{S}$ has the same length order as Kolmogorov scale. It is inferred that high-concentration fluorescent dye patch resulted from turbulent diffusion is in Kolmogorov scale.

The increase of dye patches with the small area, which is equivalent to the Kolmogorov scale order, in the other hand, dye patches with large area is coming from global expansion of the plume and increases its scale according to the Taylor's diffusion theory. As the result, scales of larger patches and of smaller patches will separated. From the consideration above, the tendency may be understood according to the developing spectrum that follows the turbulent diffusion.

Now, considering the characteristics of turbulent diffusion and its dependency on diffusion time, we can propose a source location estimation method. The proposed method takes 4 steps as follows. 1) Extract high-concentration patches from the instantaneous concentration distribution obtained at *x* by binaryzation. The patches are labeled 2) The dimensionless areas of the patches are statistically processed to obtain PDF and calculate kurtosis *Ku* of the distribution. 3) Introduce the hypothesis that the kurtosis has the linear relationship to the streamwise location *x*. 4) Based on the hypothesis, turbulent diffusion source can be estimated.

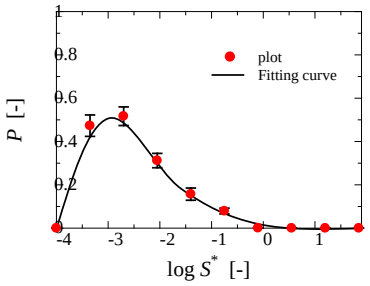

(a) T^*=10

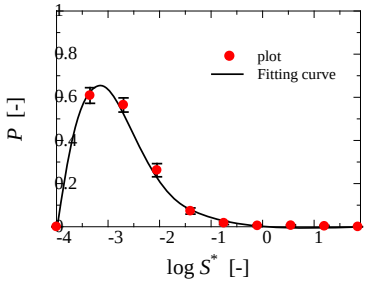

(b) T^*=30

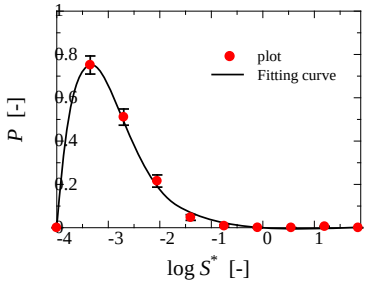

(c) T^*=60

Figure 7 Probability density function of log S^*.

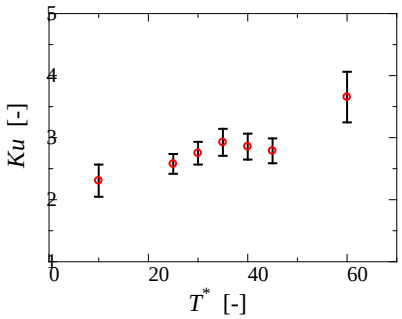

Figure 8 Kurtosis for different diffusion time.

Evaluation of proposed source location estimation method

As the proposed method is constructed based on an empirical relation Eq. (8), its availability must be verified.

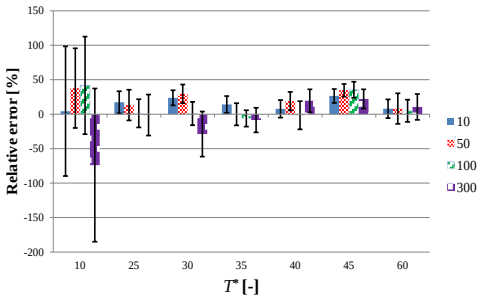

Figure 9 Relative errors for different diffusion time.

Moreover, from the chaotic nature of the turbulence, the availability of the method will be largely affected by the size of the obtained data and location where the data are taken.

To investigate the feasibility and accuracy of this method, relative errors of diffusion time are calculated for different diffusion times based on 300, 100, 50 and 10 binarized PLIF images respectively which have image data size of 0.13 megabyte per one frame, and the results are shown in Fig. 9. With different number of images applied for the same diffusion time, only very small difference is seen in the accuracy, especially for larger diffusion time such as T^*=60. Besides, a decreasing relative error occurs as the diffusion time increases, which drops to be within ±10% for T^*=60. Thus, the presented method is accurate and efficient (based on limited data) when using images obtained at locations far enough from the point source, which make it possible to be applied for practical problems.

As the result of estimation, relative error of source location is around 20% except for the location in the vicinity to the source and unaffected by the data size (i.e. number of binarized PLIF pictures) in the range of 10 to 300 instantaneous binarized pictures of instantaneous concentration distribution. On the assumption that 20% of relative error is acceptable, the proposed method is applicable to the location of T^*>25 and data size larger than 10 frames (0.13×10 megabyte).

CONCLUSIONS

In the purpose of proposing and evaluating a source location estimation method for turbulent diffusion based on limited data obtained in the downstream location, we performed image processing for the turbulent dye diffusion images, to investigate streamwise variations of the fractal dimension and the perimeter(=X^*) and square measure (=S^*) of dye patches.

Source estimation method based on limited experimental data has been successfully developed in this paper by finding a characteristic quantity linearly related with dimensionless turbulent diffusion time. In the process, experiments are conducted with PLIF technique for different diffusion time and a series of dye diffusion images are obtained, from which obvious plume expanding by turbulent diffusion in *z* direction is seen. Then, binaryzation of the raw images is performed to generate a series of binary images. Through labeling, the dye patches in each binary image are recognized, based on which the dimensionless perimeters X^* as well as areas S^* of the dye patches are calculated respectively and thus the fractal dimension of the dye patches is obtained, which however is found to be independent of diffusion time. Then the fractal dimension may be unavailable for the estimation of source location.

After that, the probability density function of log (S^*) is plotted, and the kurtosis of the PDF curves (= *Ku)* are found to be linearly related with diffusion time. Through least square method, a formulation is derived relating $T^*$and *Ku*. The feasibility and accuracy of this formulation for source estimation is studied by calculating the relative errors for cases at different diffusion time as well as different number of images. The relative errors tend to decrease as diffusion time increases, and the number of images used for estimation has little effect on the accuracy of the results. It is concluded that the proposed method based on the established T^*-*Ku* relationship can estimate the source location accurately based on limited data information collected at a far enough distance from the point source.

On the assumption that 20% of relative error is acceptable, the proposed method is applicable to the location of T^*>25 and data size larger than 10 frames (0.13×10 megabyte).

ACKNOWLEDGEMENT

I am deeply grateful to Ms. Shao Qianqian who provided the helpful comments and discussions for this study.

REFERENCES

Zhang, T. F., and Chen, Q., 2007 “Identification of contaminant sources in enclosed environments by inverse CFD modeling”, *Indoor Air*, Vol.17, pp. 167-177.

Islam, M. A., 1999, “Application of Gaussian plume model to determine the location of an unknown emission source”, *Water, Air, and Soil Pollution*, Vol. 112, pp. 241-245.

Bagtzoglou, A. C., Dougherty, D. E., and Tompson, A. F. B., 1992, “Application of Particle Methods to Reliable Identification of Groundwater Pollution Sources”, *Water Resources Management*, Vol.6, pp. 15-23.

Webster, D. P., Volyanskyy, K. Y., and Weissburg, M. J., 2011, “Sensory-mediated tracking behaviour in turbulent chemical plumes”, *Proc. of the 7th Int. Symp. on Turbulence & Shear Flow Phenomena*, Ottawa, Canada, pp. 1-6.

Oyagi, K., Tsukahara, T., and Kawaguchi, Y., 2013, “Characteristics extraction of a turbulent diffusion state for quick trace-back estimation of the diffusion source”, *Proc. of the 8th Int. Symp. on Turbulence & Shear Flow Phenomena*, Poitiers, France, PSB2 (6 pages).

Otsu, N., 1980, “An Automatic Threshold Selection Method Based on Discriminant and Least Squares Criteria”, *The Institute of Electronics, Information and Communication Engineers Journal D*, Vol.J63-D, No.4, pp. 349-356.